Electronic Supplementary Information

Influence of size, crosslinking degree and surface structure of poly(*N*-vinylcaprolactam)-based microgels on their penetration into multicellular tumor spheroids

Changchang Zhang,[‡a] Elisabeth Gau,[‡b,c] Wenjie Sun,[a] Jianzhi Zhu,[a] Ben Michael Schmidt,[b,c] Andrij Pich,*[b,c,d] Xiangyang Shi*[a]

[a] State Key Laboratory for Modification of Chemical Fiber and Polymer Materials, International Joint Laboratory for Advanced Fiber and Low-dimension Materials, College of Chemistry, Chemical Engineering and Biotechnology, Donghua University, Shanghai 201620, People's Republic of China

[b] Functional and Interactive Polymers, Institute of Technical and Macromolecular Chemistry, RWTH Aachen University, Worringerweg 2, 52074, Aachen, Germany

[c] DWI – Leibniz-Institute for Interactive Materials e.V., Forckenbeckstraße 50, 52074, Aachen, Germany

[d] Aachen Maastricht Institute for Biobased Materials (AMIBM), Maastricht University, Brightlands Chemelot Campus, Urmonderbaan 22, 6167 RD Geleen, The Netherlands

* Corresponding author. E-mail: xshi@dhu.edu.cn (X. Shi) and pich@dwi.rwth-aachen.de (A. Pich)

‡ Authors contributed equally to this work.

Part of experimental section

Materials. *N*-Vinylcaprolactam (VCL, 98%) and glycidyl methacrylate (GMA, 97%) were from Aldrich (St. Luis, MO) and distilled before use. 2-Methoxyethyl acrylate (MEA, 98 %) and di(ethylene glycol) ethyl ether acrylate (DEGA, ≥ 90 %) were also from Aldrich and passed through a basic aluminum oxide column before usage to remove the inhibitor. *N, N'*-Methylenebis(acrylamide) (BIS, 99%), 2,2'-azobis(2-methylpropionamidine) dihydrochloride (AMPA, 97%) and Pluronic F-127 were all purchased from Aldrich and used as received. Cetyltrimethylammoniumbromide (CTAB, 98%, ABCR, Karlsruhe, Germany) and the dye cyanine-3-amine (Cy3, 95%, Lumiprobe, Hannover, Germany) were used as received. AggreWell 400 plates and Ultra-low adherent 6-well plates were purchased from Stem Cell™ Technologies (Los Angeles, CA). Cell Counting Kit-8 (CCK-8) was purchased from 7Sea Biotech. Co., Ltd. (Shanghai, China). HeLa cells (a human cervical carcinoma cell line) were provided by cell resource center of Institute of Biochemistry and Cell Biology, the Chinese Academy of Sciences (Shanghai, China). Dulbecco's modified Eagle's medium (DMEM, GIBCO, Invitrogen, Carlsbad, CA), fetal bovine serum (FBS, GIBCO), penicillin-streptomycin (HyClone, Thermo Scientific, Logan, UT) and trypsin 0.25% solution (HyClone) were bought from Hangzhou Jinuo Biomedical Technology (Hangzhou, China). Water used in all experiments was purified by a RephiLe purist UV Ultrapure water system with a resistivity higher than 18.2 MΩ.cm (RephiLe Bioscience, Ltd., Shanghai, China).

Characterization. Dynamic light scattering was used to determine the hydrodynamic radius and the size distribution of the microgels. Measurements were carried out using an ALV/CGS-3 Compact Goniometer System with an ALV/LSE 5004 Tau Digital Correlator and a JDS Uniphase laser operating at 632.8 nm. A fixed scattering angle of $\theta = 90°$ was used. Before the measurements, all samples were filtered through a 1.2 μm PET filter and diluted with water until they showed no

turbidity. To investigate the colloidal stability of the microgel samples, the sedimentation velocity was determined with an analytical centrifuge LUMIFuge from L.U.M. GmbH (Berlin, Germany) at room temperature using a speed of 3000 rpm. The sedimentation velocities were calculated from the slope of the sedimentation curves (distance *vs.* time). The incorporation of the comonomers of OEGA into the microgels was investigated with Fourier transform infrared (FTIR) spectroscopy. The lyophilized samples were measured on a Thermo Nicolet Nexus 470 FTIR with Si-ATR or as KBr pellet on a Nicolet 5700 FTIR (New York, NY). Atomic force microscopy was measured with a NanoScope V from Veeco Instruments (Munich, Germany) in tapping mode. An NCH-50 POINTPROBE®-Silicon SPM-Sensor from Nanoworld with a resonance frequency of 320 kHz and a force constant of 42 N/m was used as cantilever. The recorded images were analyzed with the software Gwyddion 2.28.

Statistical Analysis. One-way analysis of variance (ANOVA) method was used to evaluate the significance of the experimental data with a significance level (p value) of 0.05. The data were marked with (*) for $p < 0.05$, (**) for $p < 0.01$, (***) for $p < 0.001$, respectively. All experimental data were displayed as the mean ± standard deviation ($n \geq 3$).

Part of results and discussion

Table S1. Amounts of monomers, stabilizer, crosslinker and reaction temperature for the PVCL/OEGA/GMA microgel synthesis. Each sample contained 5 mol% of GMA.

#	desired R_h [nm]	monomer amount [mmol]	n (VCL) [mmol]	OEGA content [mol%]	n (OEGA) [mmol]	m (CTAB) [mg]	BIS [mol%]	T [°C]
1	100	15	11.25	MEA, 20	3.00	9.6	2.5	70
2	200	15	11.25	MEA, 20	3.00	1.6	2.5	70
3	300	15	11.25	MEA, 20	3.00	---	2.5	70
4	400	17.5	13.13	MEA, 20	3.50	---	2.5	60
5	500	20	15.00	MEA, 20	4.00	---	2.5	60
6	200	15	11.25	MEA, 20	3.00	1.4	0.5	70
7	200	15	11.25	MEA, 20	3.00	2.4	1.0	70
8	200	15	13.50	MEA, 5	0.75	4.0	2.5	70
9	200	15	12.75	MEA, 10	1.50	3.6	2.5	70
10	200	15	9.75	MEA, 30	4.50	1.0	2.5	70
11	200	15	11.25	DEGA, 20	3.00	1.0	2.5	70

Regulation of different PVCL/OEGA/GMA microgels

Variation of the microgel size

Table S2. Reaction parameters (monomer amount, reaction temperature and CTAB concentration) as well as hydrodynamic radii and polydispersity index (PDI) values at 20 °C and 50 °C of the PVCL/$MEA_{20\ mol\%}$/$GMA_{5\ mol\%}$ microgels with different sizes used for the tumor penetration studies.

#	monomer amount [mmol]	react. temp. [°C]	CTAB concentration [mg/L]	R_h (20 °C) [nm]	PDI (20 °C)	R_h (50 °C) [nm]	PDI (50 °C)
1	100	70	64.0	88.9 ± 2.8	0.085	55.8 ± 0.7	0.019
2	100	70	10.7	209.0 ± 11.4	0.067	126.5 ± 1.6	0.030
3	100	70	0	297.1 ± 8.0	0.072	169.9 ± 0.7	0.041
4	117	60	0	370.5 ± 18.5	0.128	151.4 ± 0.6	0.160
5	133	60	0	477.6 ± 29.4	0.161	165.7 ± 3.3	0.139

Table S3. Yields, zeta potentials and sedimentation velocities of the PVCL/$MEA_{20\ mol\%}$/$GMA_{5\ mol\%}$ microgels with different sizes for the tumor penetration studies.

#	desired R_h [nm]	solid content [mg/mL]	yield [%]	zeta potential [mV]	sedimentation velocity [µm/s]
1	100	11.0	76.2	3.6 ± 0.3	1.32 ± 0.00
2	200	12.9	88.8	4.5 ± 0.1	1.30 ± 0.02
3	300	13.8	95.3	3.6 ± 0.2	3.21 ± 0.03
4	400	13.2	78.2	2.1 ± 0.1	3.82 ± 0.08
5	500	17.0	88.8	0.5 ± 0.1	4.13 ± 0.01

Variation of the crosslinking density

Table S4. Reaction parameters (monomer amount, crosslinker content and CTAB concentration) as well as hydrodynamic radii and PDI values at 20 °C and 50 °C of the PVCL/$MEA_{20\ mol\%}$/$GMA_{5\ mol\%}$ microgels with different crosslinking densities for the tumor penetration studies.

#	monomer amount [mmol]	x (BIS) [mol%]	CTAB concentration [mg/L]	R_h (20 °C) [nm]	PDI (20 °C)	R_h (50 °C) [nm]	PDI (50 °C)
6	100	0.5	9.33	223.3 ± 1.6	0.072	108.6 ± 1.5	0.048
7	100	1.0	16.0	188.8 ± 3.3	0.084	97.2 ± 0.3	0.069
2	100	2.5	10.7	209.0 ± 11.4	0.067	126.5 ± 1.6	0.030

Table S5. Yields, zeta potentials and sedimentation velocities of the PVCL/$MEA_{20\ mol\%}$/$GMA_{5\ mol\%}$ microgels with different crosslinking densities for the tumor penetration studies.

#	crosslinker content [mol%]	solid content [mg/mL]	yield [%]	zeta potential [mV]	sedimentation velocity [µm/s]
6	0.5	13.6	96.2	3.1 ± 0.1	0.63 ± 0.01
7	1.0	13.1	92.2	5.1 ± 0.3	0.63 ± 0.00
2	2.5	12.9	88.8	4.5 ± 0.1	1.30 ± 0.02

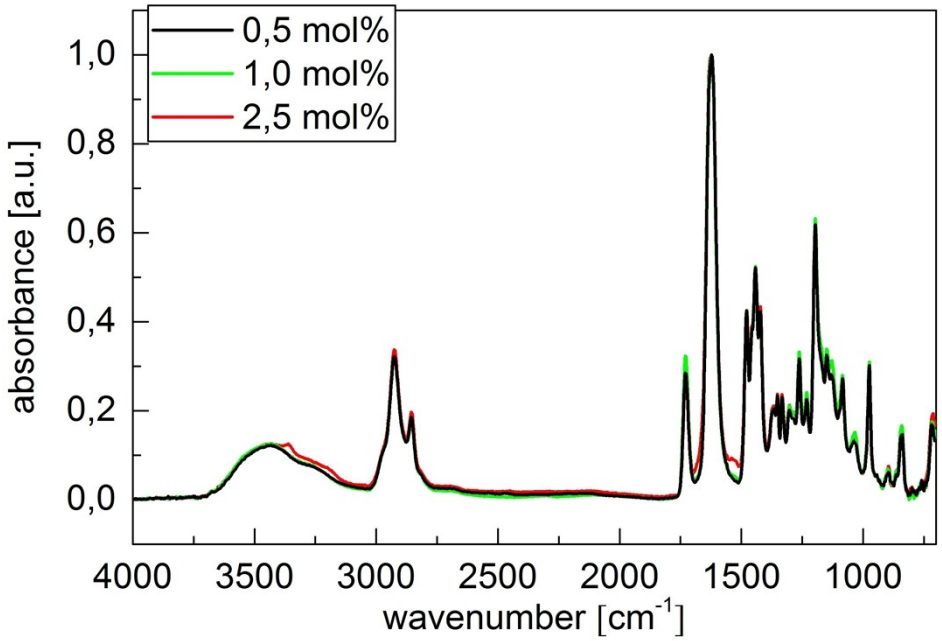

Fig. S1 FTIR spectra of PVCL/$MEA_{20\ mol\%}$/$GMA_{5\ mol\%}$ microgels with different crosslinking densities (0.5 mol%, 1.0 mol% and 2.5 mol%, respectively).

Variation of the MEA comonomer content

Table S6. Reaction parameters (monomer amount, MEA content and CTAB concentration) as well as hydrodynamic radii and PDI values at 20 °C and 50 °C of the PVCL/$MEA_{20\ mol\%}$/$GMA_{5\ mol\%}$ microgels with different MEA contents used for the tumor penetration studies.

#	monomer amount [mmol]	MEA content [mol%]	CTAB concentration [mg/L]	R_h (20 °C) [nm]	PDI (20 °C)	R_h (50 °C) [nm]	PDI (50 °C)
8	100	5	26.7	212.5 ± 2.5	0.032	102.7 ± 0.2	0.035
9	100	10	24.0	191.1 ± 1.3	0.080	92.9 ± 0.5	0.036
2	100	20	10.7	209.0 ± 11.4	0.067	126.5 ± 1.6	0.030
10	100	30	6.7	202.4 ± 9.2	0.225	140.3 ± 0.7	0.179

Table S7. Yields, zeta potentials and sedimentation velocities of the PVCL/MEA/$GMA_{5\ mol\%}$ microgels with different MEA contents for the tumor penetration studies.

#	MEA content [mol%]	solid content [mg/mL]	yield [%]	zeta potential [mV]	sedimentation velocity [µm/s]
8	5.0	14.1	96.3	0.3 ± 0.1	0.34 ± 0.00
9	10.0	13.2	90.4	5.9 ± 0.1	0.33 ± 0.00
2	20.0	12.9	88.8	4.5 ± 0.1	1.30 ± 0.02
10	30.0	10.2	70.9	9.7 ± 0.1	6.03 ± 0.21

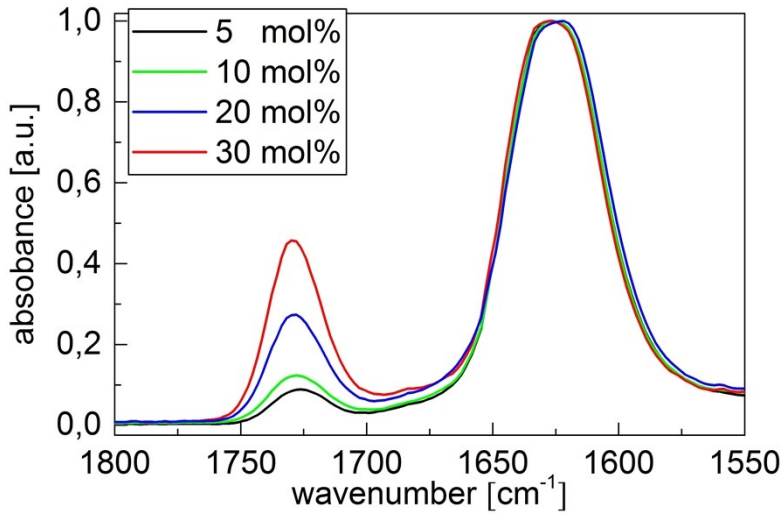

Fig. S2 FTIR spectra of the PVCL/MEA/$GMA_{5\ mol\%}$ microgels with different MEA contents. The characteristic band from the C=O stretching vibration of the MEA at 1730 cm^{-1} increases with increasing MEA content.

Variation of the OEGA chain length

Table S8. Reaction parameters (monomer amount, OEGA type and content and CTAB concentration) as well as hydrodynamic radii and PDI values for 20 °C and 50 °C for the PVCL/OEGA/$GMA_{5\ mol\%}$ microgels used in the tumor penetration studies.

#	monomer amount [mmol]	OEGA [mol%]	CTAB concentration [mg/L]	R_h (20 °C) [nm]	PDI (20 °C)	R_h (50 °C) [nm]	PDI (50 °C)
2	100	MEA 20	10.7	209.0 ± 11.4	0.067	126.5 ± 1.6	0.030
11	100	DEGA 20	6.67	175.5 ± 9,7	0.047	109.6 ± 1.6	0.055

Table S9. Yields, zeta potentials and sedimentation velocities of the PVCL/$OEGA_{20\ mol\%}$/$GMA_{5\ mol\%}$ microgels with OEGAs of different chain lengths for the tumor penetration studies.

#	OEGA [mol%]	solid content [mg/mL]	yield [%]	zeta potential [mV]	sedimentation velocity [µm/s]
2	MEA-20	12.9	88.8	4.5 ± 0.1	1.30 ± 0.02
11	DEGA-20	13.6	86.7	9.8 ± 0.2	1.16 ± 0.01

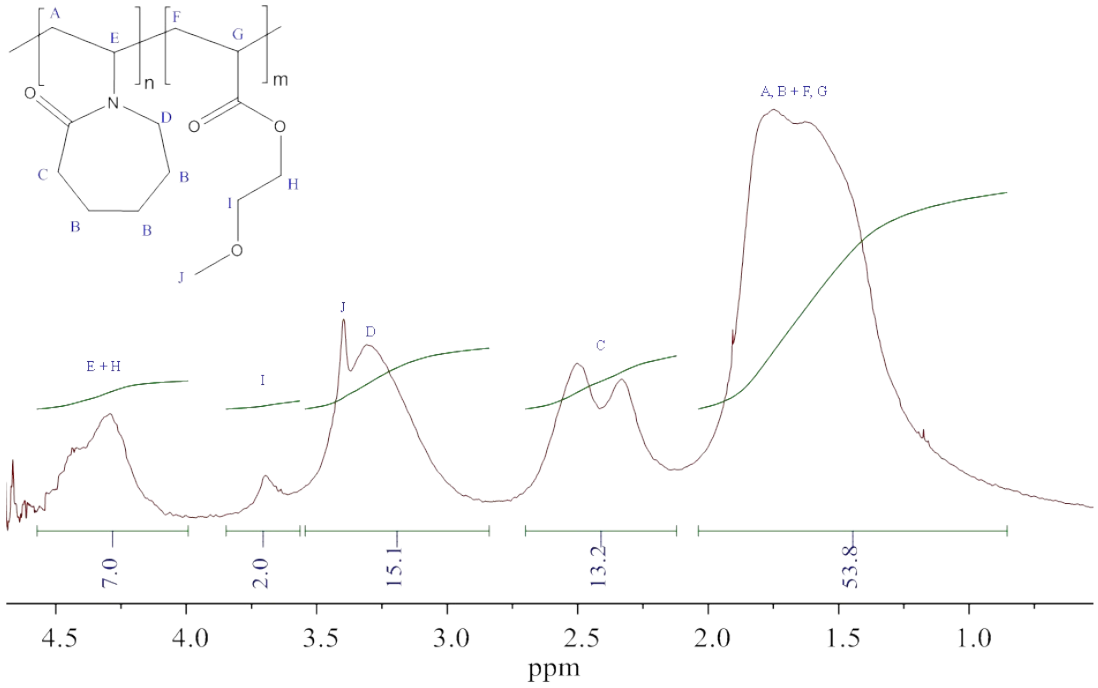

Fig. S3 ^{1}H-NMR spectrum of the PVCL/MEA$_{20\ mol\%}$/GMA$_{5\ mol\%}$ microgels. Signals for the GMA cannot be observed due to the too low content.

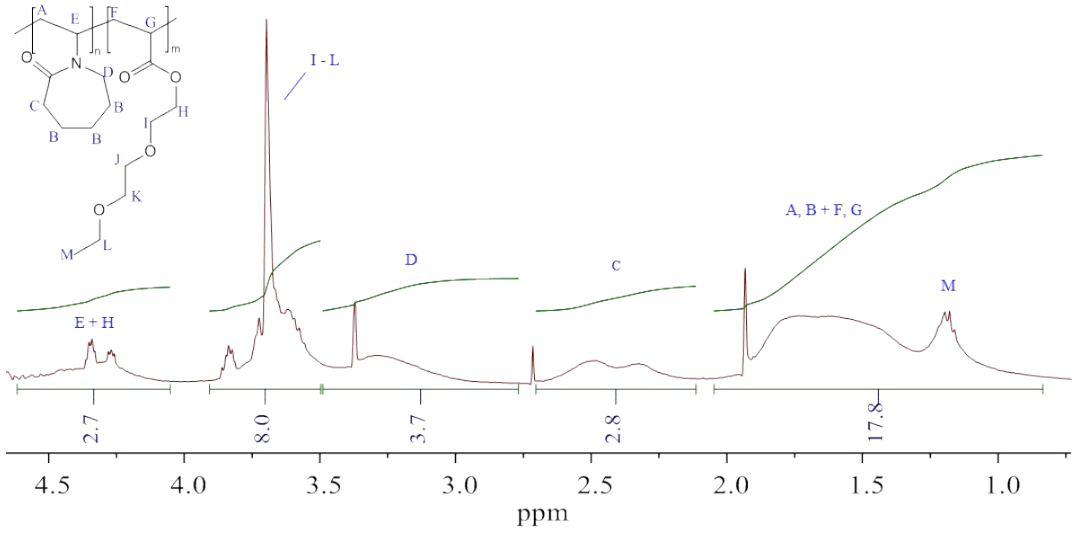

Fig. S4 ^{1}H-NMR spectrum of the PVCL/DEGA$_{20\ mol\%}$/GMA$_{5\ mol\%}$ microgels. Signals for the GMA cannot be observed due to the too low content.

Covalent attachment of Cyanine-3-amine dye and *in vitro* penetration study

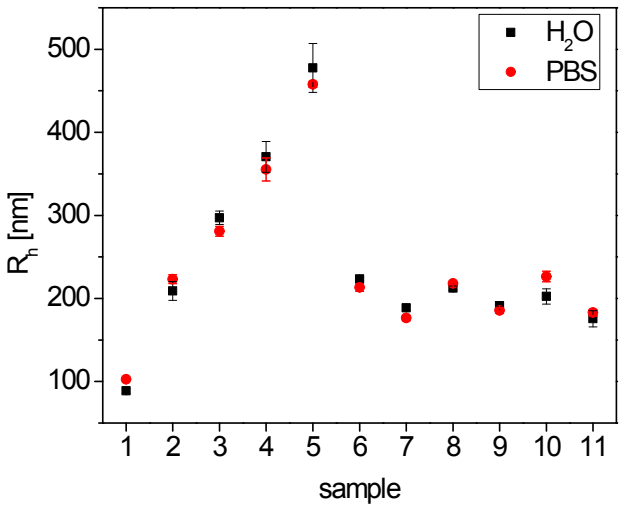

Fig. S5 Comparison of the hydrodynamic radii of all PVCL/OEGA/GMA microgels in water and in PBS (10 mM, pH = 7.4) at 20 °C.

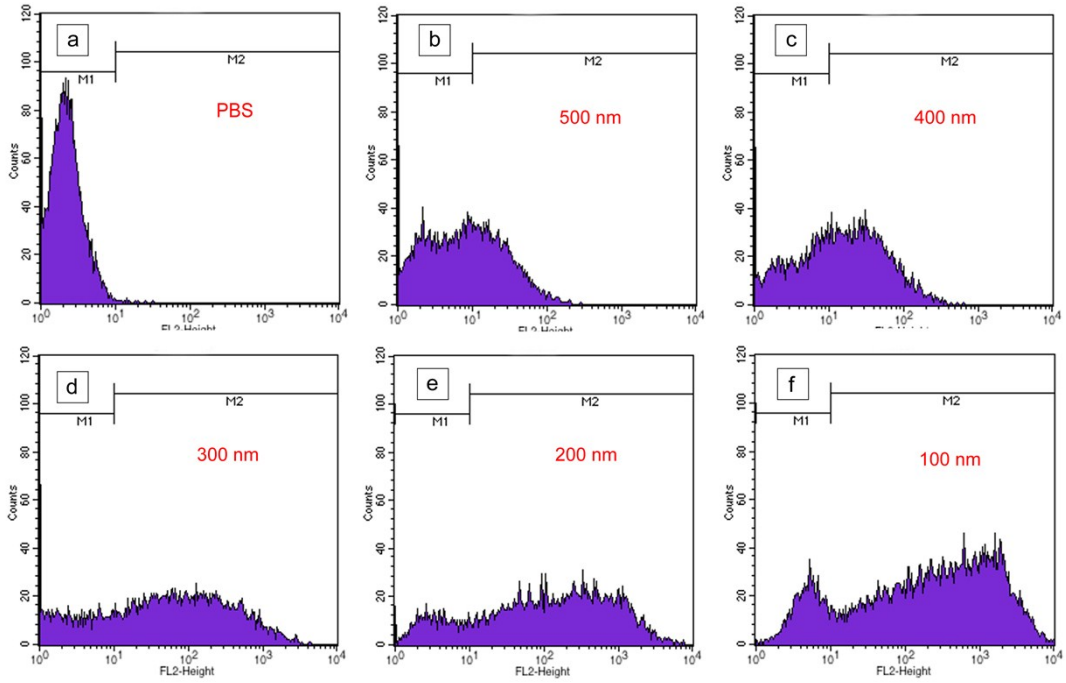

Fig. S6 Flow cytometric analysis of HeLa cells treated with PBS **(a)**, and Cy3-labeled microgels with different radii **(b, c, d, e, f)** at a microgel concentration of 100 μg/mL for 4 h.

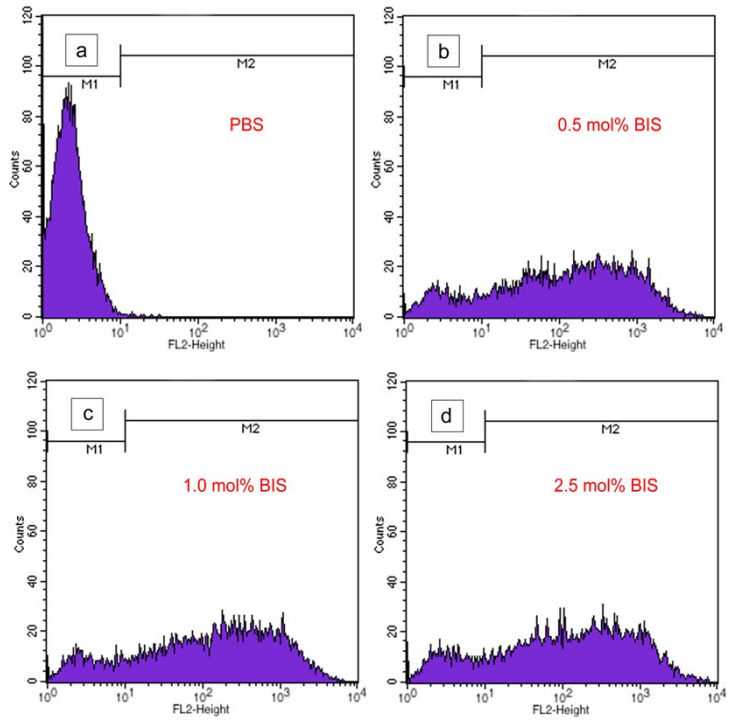

Fig. S7 Flow cytometric analysis of HeLa cells treated with PBS **(a)**, and Cy3-labeled microgels with different BIS concentrations **(b, c, d)** at a microgel concentration of 100 μg/mL for 4 h.

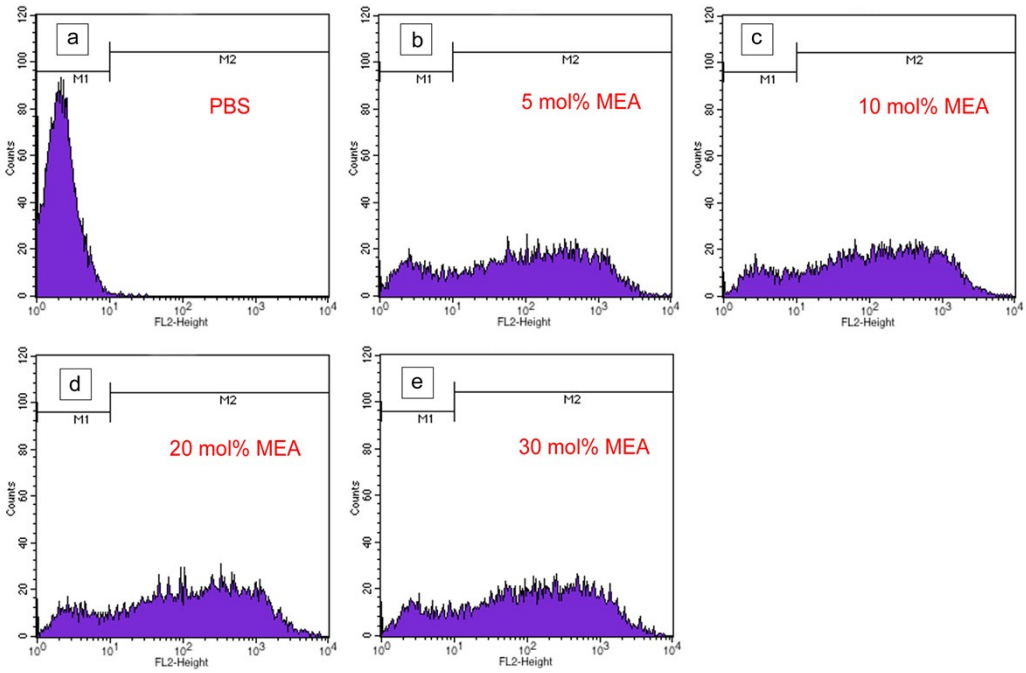

Fig. S8 Flow cytometric analysis of HeLa cells treated with PBS **(a)**, and Cy3-labeled PVCL microgels with different MEA concentrations **(b, c, d, e)** at a microgel concentration of 100 μg/mL for 4 h.

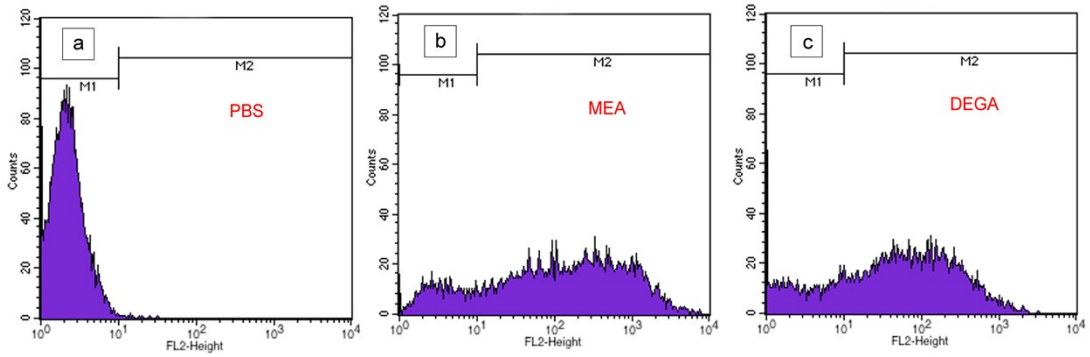

Fig. S9 Flow cytometric analysis of HeLa cells treated with PBS **(a)**, and Cy3-labeled PVCL microgels with different OEGA monomers **(b, c)** at a microgel concentration of 100 μg/mL for 4 h.

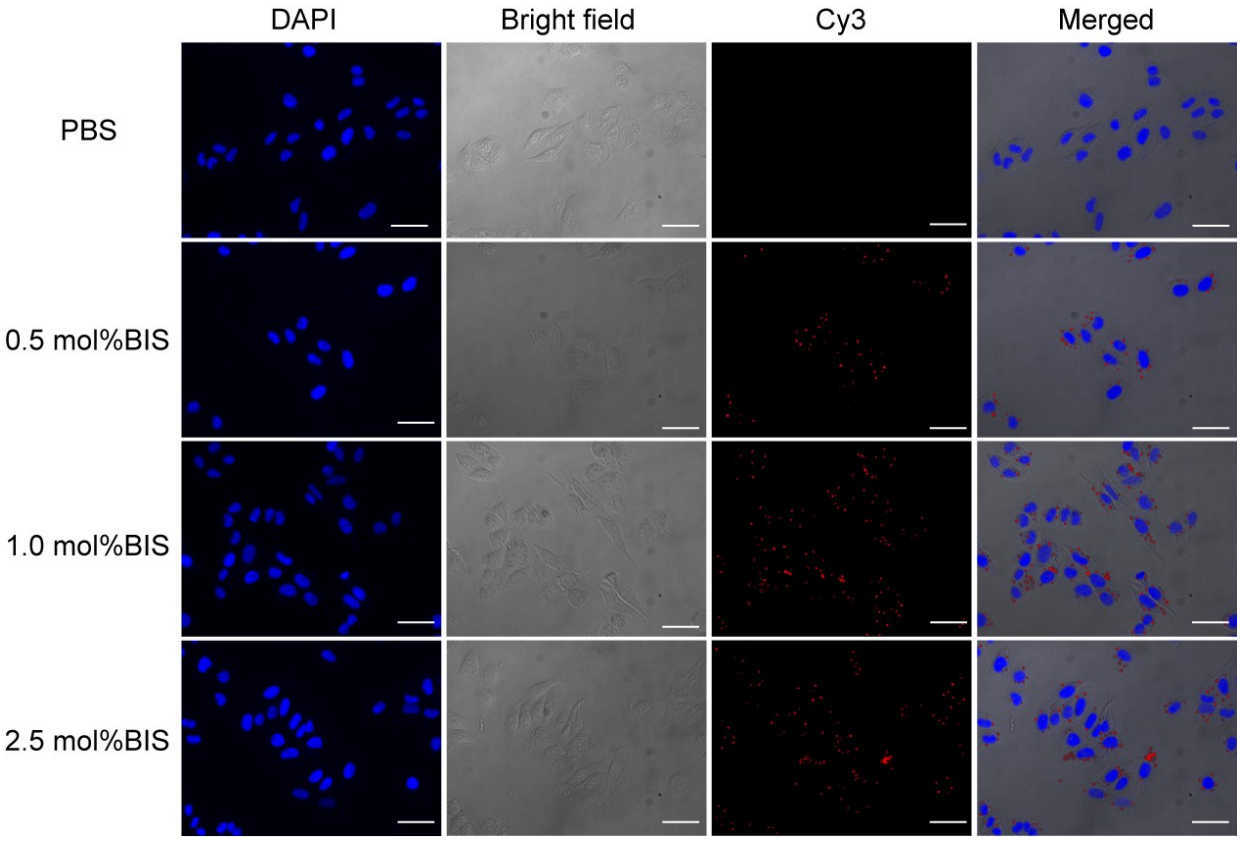

Fig. S10 Fluorescence microscopic images of HeLa cells incubated with PBS, Cy3-labeled microgels with different crosslinking densities at a microgel concentration of 100 μg/mL for 4 h, respectively. The cell nuclei were stained with DAPI. Scale bar in each panel represents 50 μm.

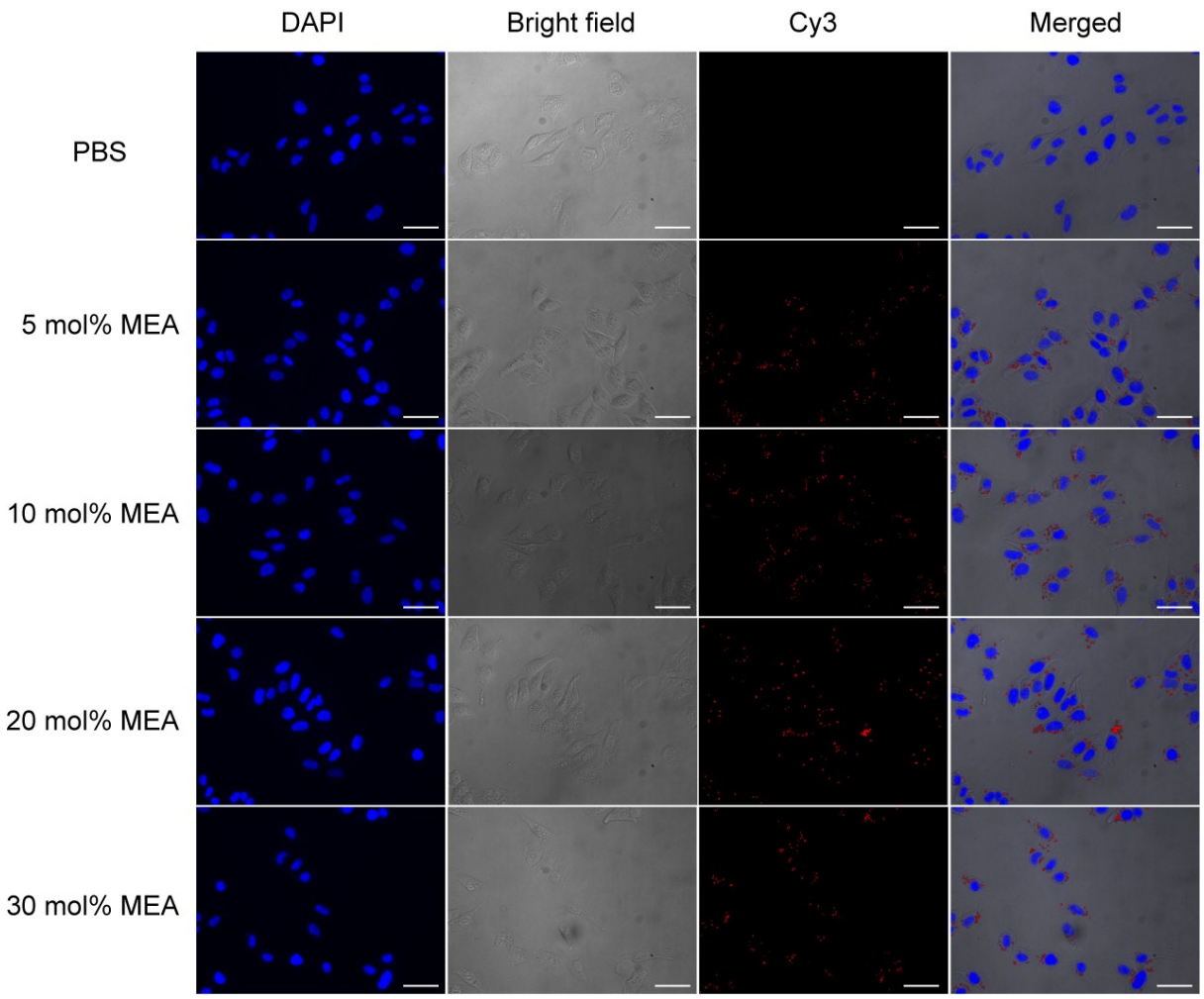

Fig. S11 Fluorescence microscopic images of HeLa cells incubated with PBS, Cy3-labeled microgels with different MEA contents at a microgel concentration of 100 μg/mL for 4 h, respectively. The cell nuclei were stained with DAPI. Scale bar in each panel represents 50 μm.

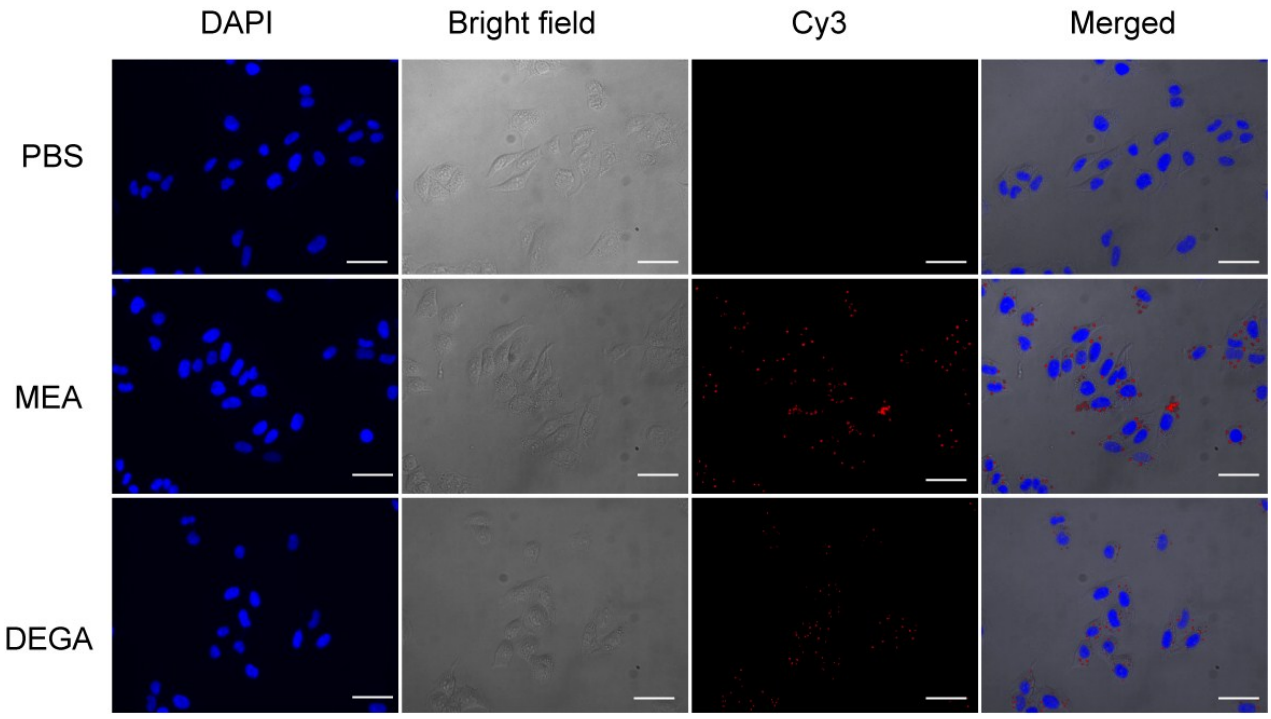

Fig. S12 Fluorescence microscopic images of HeLa cells incubated with PBS, Cy3-labeled microgels with different OEGA comonomers at a microgel concentration of 100 μg/mL for 4 h, respectively. The cell nuclei were stained with DAPI. Scale bar in each panel represents 50 μm.

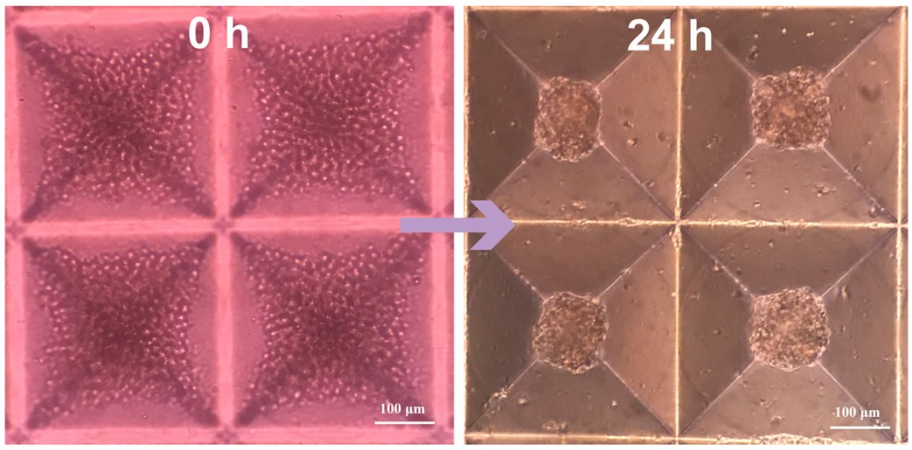

Figure S13. MCTs formation in Aggrewell™.

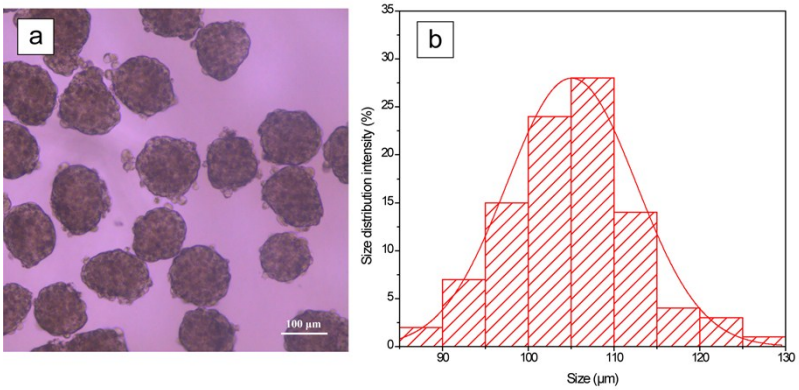

Fig. S14 Phase contrast microscopic images of HeLa MCTs: **(a)** MCTs in ultra-low attachment plates; **(b)** the size distribution histogram of MCTs.

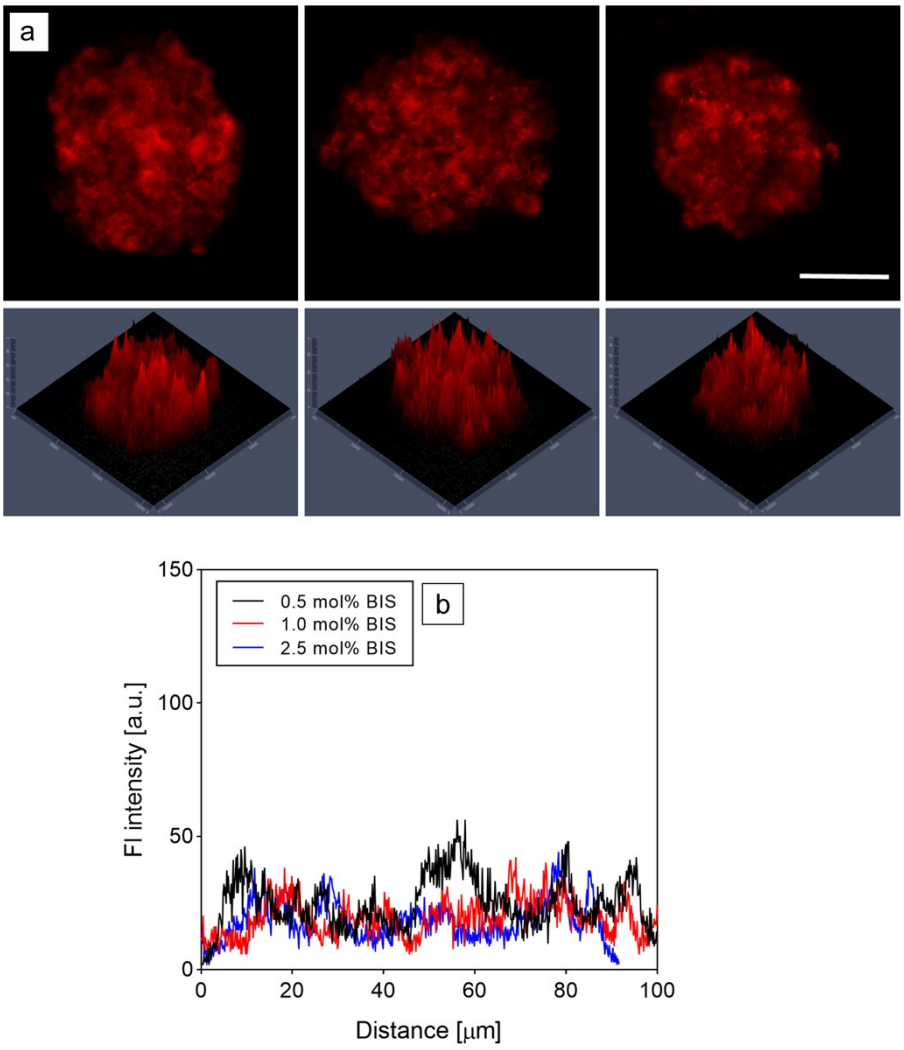

Fig. S15 (a) CLSM images of HeLa MCTs incubated with PVCL microgels with different BIS concentrations (0.5, 1 and 2.5%, respectively) at a microgel concentration of 300 μg/mL for 6 h. Scale bar in each panel represents 50 μm. **(b)** Fluorescence intensity of HeLa MCTs incubated with the Cy3-labeled PVCL microgels.

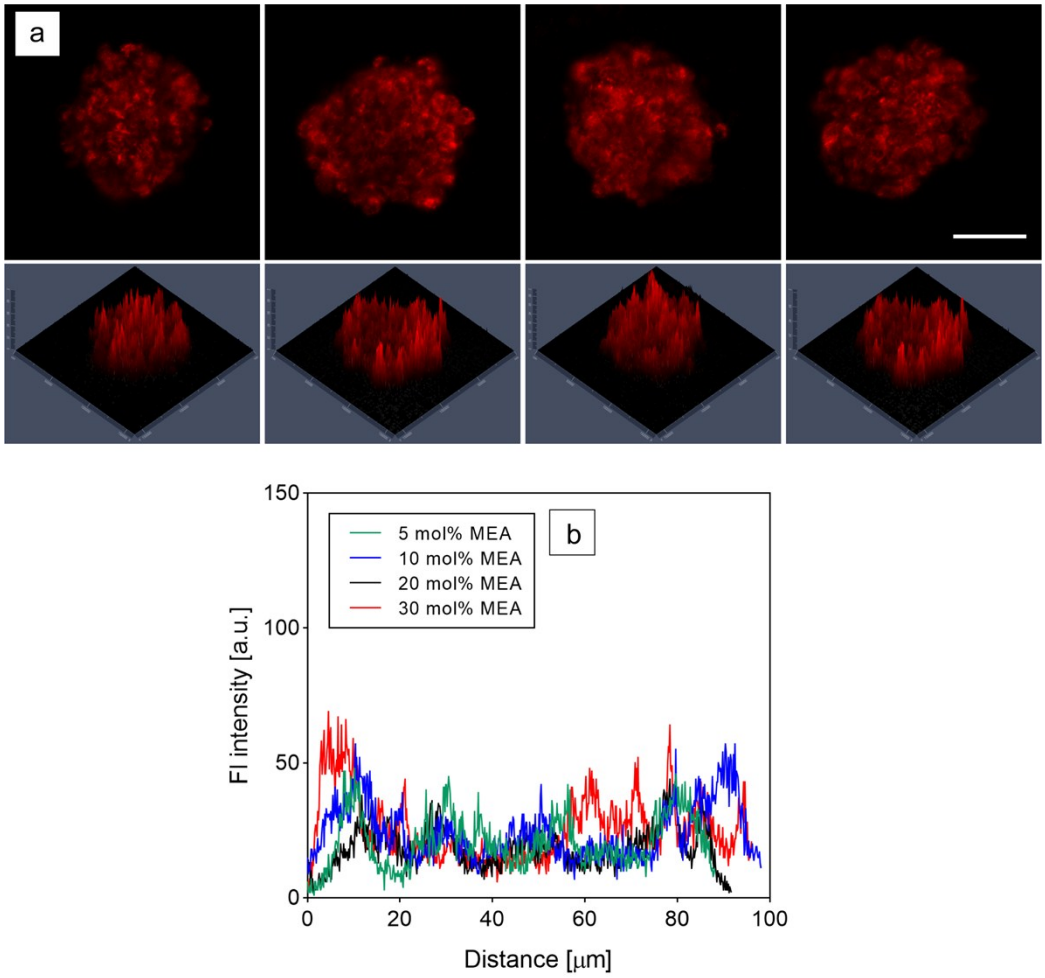

Fig. S16 (a) CLSM images of HeLa MCTs incubated with PVCL microgels with different MEA concentrations (5, 10, 20 and 30%, respectively) at a microgel concentration of 300 μg/mL for 6 h. Scale bar in each panel represents 50 μm. **(b)** Fluorescence intensity of HeLa MCTs incubated with the Cy3-labeled PVCL microgels.

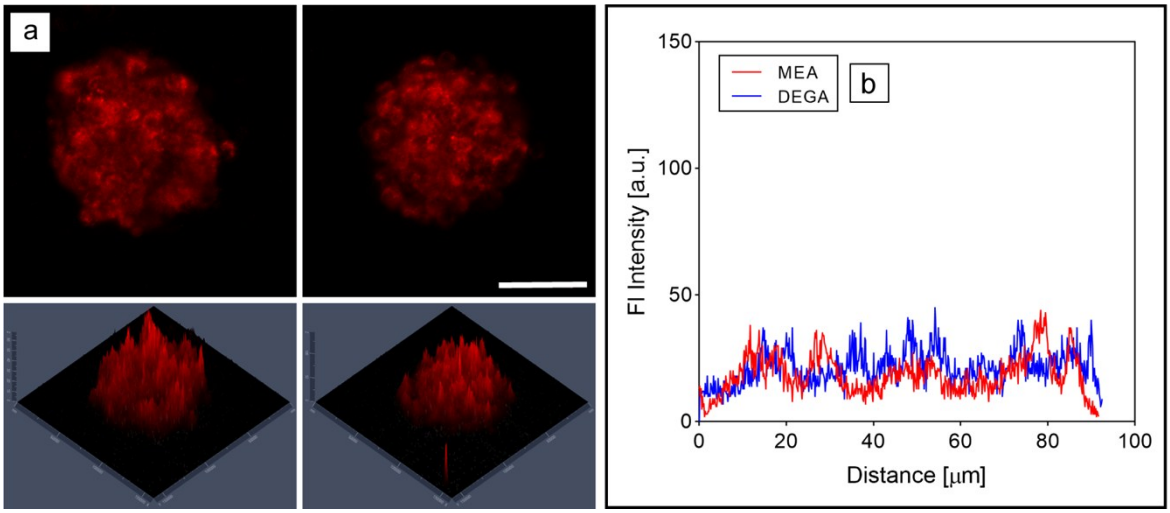

Fig. S17 (a) CLSM images of HeLa MCTs incubated with PVCL microgels with different OEGA comonomers (MEA and DEGA) at a microgel concentration of 300 μg/mL for 6 h. Scale bar in each panel represents 50 μm. **(b)** Fluorescence intensity of HeLa MCTs incubated with the Cy3-labeled PVCL microgels.